SUPPLEMENTAL INFORMATION

Table S1, Genotypes of flies used in this study, related to STAR Methods.

Table S2, Oligonucleotides used in this study, related to STAR Methods.

Supplemental Figure Legends

Figure S1. Expression and localization of DIP-α, Dpr6 and Dpr10 proteins throughout visual system development. Related to Figure 1. (A-F) Antibody staining for DIP-α, Dpr6 and Dpr10 during pupal development as indicated. Monoclonal antibody staining to DIPα and Dpr6, and polyclonal antibody to Dpr10 were used in whole mount wild-type optic lobes in A-C'''. (D-F) DIPα, Dpr6, and Dpr10 antibody staining in control null allele of DIP-α, Dpr6 and Dpr10, respectively. Medulla neuropil is encircled with red dashed line.

Figure S2. Dm4 and Dm12 processes overlap in the developing M3 layer. Related to Figure 1. (A-A'') Overlap of Dm4 process labeled with Dm4-GAL4/UAS-myrGFP labeled Dm4 and Dpr6 protein detected with anti-Dpr6 antibody. See Figure S1 for control staining in *dpr6* mutant. Arrows, Dm4 terminals in incipient M3. (B-B') Co-localization of Dm12 and Dm4 processes in incipient M3. Dm4, 75F06-lexA/ LexAop-myrtdTomato and 84A12-GAL4/UAS-myr-GFP. The green label is weak; Dm12, 84A12-GAL4/UAS-myrGFP, only. As a result, Dm4 is labeled by both red and green (arrowhead), while Dm12 is labeled by green (arrow). Separate green processes (Dm12) and red processes with weak green staining (Dm4) show overlapping patterns.

Figure S3. Dpr6- and Dpr10-GAL4 label many lamina and medulla neurons at 40hrs APF. Related to Figure 1. (A) Dpr6-GAL4 driving UAS-myrGFP in the optic lobe at 40hrs APF; (B) Dpr10-GAL4 driving UAS-myrGFP in the optic lobe at 40hrs APF.

Figure S4. R7 targeting and presynaptic number in *dpr11*^{null} mutants is normal. Related to Figure 2. (A-B) yR7 terminals analyzed by STaR. (A) Left panel, wild type yR7 neurons (n=275/4 animals); Right panel, *dpr11*^{null} mutant R7 neurons (n=281/4 animals). Arrowhead, R7 overshoot phenotype. (B) The difference in yR7 overshoot phenotypes between wild-type and *dpr11*^{null} mutants is not significant ($p = 0.4882$, N-1 Chi-Square test). This is in contrast to defects reported by Carillo and colleagues (Carrillo et al., 2015); (C, D). (C) Visualization of presynaptic sites (i.e. Brp puncta, green) in wild-type (Left panel) and *dpr11*^{null} mutants (Right panel). (D) No difference was seen in the number of presynaptic sites between wild-type and *dpr11*^{null} mutant R7 neurons ($p = 0.3894$, unpaired t-test). Panel D is represented as mean ± SD.

Figure S5. DIP-α regulates branch point number in Dm1. Related to Figure 2.

DIP-α null mutant clones were generated in Dm1 neurons using MARCM (A, B) and STaR/MARCM (C, D). Mutant Dm1 neurons show a reduction in branch points (arrows) (A, B, E), but no change in Brp puncta number (C, D, F). Panel E and F are represented as mean ± SD.

Figure S6. Expression of DIP-α and Dpr10 binding deficient mutants at 40h APF. Related to Figure 2, 4 and 6. (A-C') DIP-α antibody staining of wild-type (Left) and *DIP-α*^{null} mutants (Right). ; (B) DIP-α antibody staining of DIP-α^{null}/+ (Left) and *DIP-α*$^{het\text{-}homo}$ (Right); (C) DIP-α antibody staining of wild-type (Left) and *DIP-α*^{homo} (Right); and (D) Dpr10 antibody staining of wild type (Left) and *dpr10*^{het} (Right). Mutant alleles: het-homo, mutation disrupts both

heterophilic and homophilic binding; homo, mutation disrupts homophilic binding only; and het mutations only affect the binding site in Dpr10 for DIP-α. White rectangle in panel A, medulla; arrow, M3 layer; Schematics, K_D value for indicated protein-protein interaction.

Figure S7. Ectopic expression of Dpr6,10 promotes mistargeting of Dm4 terminals and relies on interactions with DIP-α. Related to Figure 3. (A, A') T4 GAL4 drives expression in the incipient M10 layer (lower dotted line). At this stage in development there is a gradient of circuit maturation with the oldest medulla neurons located to the left. Younger Dm4 neurons extending axons into the incipient M3 layer are closer to incipient M10 layer marked by the expression of Dpr10 within this layer (green speckled staining). (B-D'') The genotypes of each of the mistargeting experiments is shown above the three panels documenting the results. (B-C") Mistargeting driven by Dpr10D expression in T4 (blue) is suppressed by DIP-$\alpha^{het\text{-}homo}$, but not by *DIP-*α^{homo}. (D) Dm4 Targeting to M3 in wild-type; (D') Targeting to M3 is normal in *dpr6*, *dpr10* double mutant animals; and (D'') T4-GAL4 driving expression of UAS-Dpr6 in the developing M10 layer in a *dpr6*,*dpr10* double mutant animal re-targets Dm4 (red). Blue, anti-Dpr6 or Dpr10 antibody as indicated in figures; Red, myr-tdTomato labeled Dm4. Scale bar: 10 μm.

Figure S8. *Dpr10-RD* is the dominant mRNA isoform during pupa development. Related to Figure 3. *Dpr10-RA* and *Dpr10-RD* corresponding to the two protein isoforms of Dpr 10 (Dpr10-PA and Dpr10-PD) are shown. *Dpr10-RD* lacks one exon compared to *Dpr10-RA*. Positions of *dpr10* PCR primers are indicated (red). RNA was isolated from 3rd instar and from pupal brains at 24h, 42h, and 72h APF and analyzed by RT-PCR. Actin primers used as a

control. Dpr10-RD, referred to in the text as Dpr10D, was the predominant form expressed at all stages. Dpr10-RA was not detected.

Figure S9. Analysis of cell death in DIP-α mutants. Related to Figure 5. (A) Left, Labeled Dm4 cells generated by MARCM with different genotypes. There is a selection against *DIP–α* and *DIP-α*$^{\text{het-homo}}$ neurons generated compared to *wild-type* or *DIP-α*^{homo} neurons; Right, Wild-type and *DIP-α* overexpressing Dm4 MARCM clones. There is a selection for cells expressing higher levels of DIP-α (UAS-DIP-α driven by DIP–α-GAL4). (B) Cell number quantification of Dm12 in adult whole animal *DIP-α*^{null} , Dpr6 and Dpr10 mutants. (C) Dm4 cell loss can be prevented by overexpressing anti-apoptotic proteins Diap1 or P35 in cells normally expressing DIP-α. Error bars in (A-C) are constructed using one standard deviation from the mean. **p<0.001; *** p<0.0001. (D, E) Proliferating cells do not express DIP-α in third-instar larvae. (D, D') S-phase marker BrdU (red) does not overlap with GFP-driven by DIP-α-GAL4 (green). (E,E') A mitotic marker, phospho-Histone H3 (PH3) (red), does not overlap with GFP-driven by DIP-α-GAL4 (green) expressing cells. (D', E') are magnified views of boxed areas in D and E. Scale bar, 20μm. (F) Expression patterns of hid-GFP, rpr-lacZ and Grim Mi03811 in *DIP-α* mutant pupae at 24hrs APF. Medulla cortex is marked by white dashed lines. *hid-GFP* was seen both in lamina (yellow arrowhead) and throughout the medulla including the posterior region where developing Dm4 cell bodies are located (arrow); *rpr-lacZ* was only seen in lamina (yellow arrowhead); GrimMi03811 was seen only in medulla (including posterior medulla, arrow), but not in lamina (yellow arrowhead). (G) Grim Mi03811 signal is also seen in Dm4 neurons in *DIP-α* mutant, although the percentage of Dm4 with Grim Mi03811 positive signal is similar to wild-type (see Figure 5G). (H, I) The decrease in cell number in DIP-α is partially suppressed by removing a segment of DNA using the H99 deficiency or a single copy of *hid*. Dm4 cell number in adult *DIP-α* mutants is not affected by deficiencies removing one copy of *grim*, or outside of the H99 locus. (I) Red parentheses with a cross indicate which part of the genome is deleted in each deficiency line. Panel A, B, C and H are represented as mean ± SD.

Figure S10. Related to Figure 5. (A) Dm4 arbor coverage in wild-type neurons, DIP-α mutant neurons and DIP-α mutant neurons overexpressing Diap1; (B) Comparison of mistargeting of

Dm12 in DIP-α mutant MARCM and DIP-α mutant neurons expressing P35; (C) Brp density at M3 layer in a wild-type Dm12 within a wild type background and a DIP-α mutant Dm12 neuron within a mutant background. All panels are represented as mean ± SD.

Figure S11. A DIP requirement for Dm1 and Dm8 survival. Related to Figure 5.

(A) Cell number quantification of Dm1 in adult whole animal null mutants. (B) Cell number quantification of Dm8 in adult *DIP-γ* and *dpr11* whole animal null mutants. Note that only a subset of Dm8 axons express *DIP-γ* and thus are affected by it. We have quantified the effect on the entire population. Thus, this is an under-representation of the requirement for *DIP-γ* in *DIP-γ* -expressing neurons. Both panels are represented as mean ± SD. Error bars are constructed using one standard deviation from the mean. *** $p<0.0001$.

Figure S12. Characterization of nectin and DIP/Dpr chimeras. Related to Figure 6. (A) Similar geometry of interacting interfaces of the Ig1 domains of nectin-1 and DIP/Dpr complexes. (B) SPR binding experiments. Surface-immobilized ligands are indicated at left, and analytes across the top. No binding was observed between either chimera, nor native DIP-α or Dpr10. Binding is observed between DIP-$\alpha^{Nectin1}$ and Dpr10^{Nectin3}, as well as the homophilic interaction between DIP-$\alpha^{Nectin1}$ molecules. The K_D for heterophilic binding between chimeric proteins was calculated using the binding isotherm. (C-F) DIP-$\alpha^{Nectin1}$ protein from the knock-in allele is expressed and localized similarly to wild-type DIP-α protein. Antibodies to DIP-α (C, D) and Nectin1 (E, F) detect the chimeras in the medulla neuropil in wild-type (C, E) and DIP-$\alpha^{Nectin1}$ (D, F) knock-in pupae at 24 hrs APF. Neuropil structure is labeled with phalloidin (magenta) to visualize the protein localization pattern. The source of background cortical staining with anti-Nectin1 in wild-type is not known. Note using the DIP-α antibody that DIP-$\alpha^{Nectin1}$ is expressed in a similar level and distribution to wild-type. Arrows mark the DIP-α and DIP-$\alpha^{Nectin1}$ in nascent M3 layer. The asterisk indicates that additional mutations (L116E, Y172K) were included to stabilize the chimeric protein. Scale bar: 10 μm.

Figure S13. DIP-α homophilic interactions can cause Dm4 mistargeting to the lobula. Related to Figure 6. A and B are two examples of wild-type Dm4 targeting patterns (notice that Dm4-driver also labels some lobula neurons; the strong labeling of these neurons in panels C and D (compared to A and B) is a consequence of selectively enhancing the brightness in C and D to better visualize the axons indicated by the arrows; C and D are two examples showing Dm4 targeting patterns in *dpr6,dpr10* double mutants that express UAS-DIP-α driven by T4-GAL4. Red labels Dm4 neurons at 48h APF; arrows label small number of Dm4 axonal processes extending into the lobula. Images are maximum intensity projection of 15-20 μm Z-stack.

Figure S14. Expression of interacting DIP-Dpr proteins in synaptic partners. Direction of arrows is from pre to postsynaptic neurons. Only interacting DIPs and Dprs expressed between synaptic partners are shown. DIPs expressed in medulla neurons are in red. Synaptic partner assignments are from Takemura et al., (Takemura et al., 2013, 2015) and S. Takemura, I. Meinertzhagen, and L. Scheffer (personal communication). Dprs expressed in lamina neurons are in green. DIP expression is taken from the MCFO data in the accompanying paper (Cosmanescu et al. 2018). Expression data of Dprs are from both RNA-seq and MiMIC-derived reporters (Tan et al., 2015). The Dpr expression patterns show cell-type and temporal specificity. Here, we have only represented the cell-type specific pattern. Dpr expression in different lamina neurons is dynamic. As synapse formation occurs during a broad temporal window encompassing the second half of pupal development, different Dprs may promote interactions between DIPs expressed on different neuron types at discrete times during this period. While these representations are speculative, we present them here as it was this type of analysis that led us to

consider the possibility of phenotypes in DIP-α and Dpr6/10 mutants in Dm4 and Dm12 neurons.

Figure S1

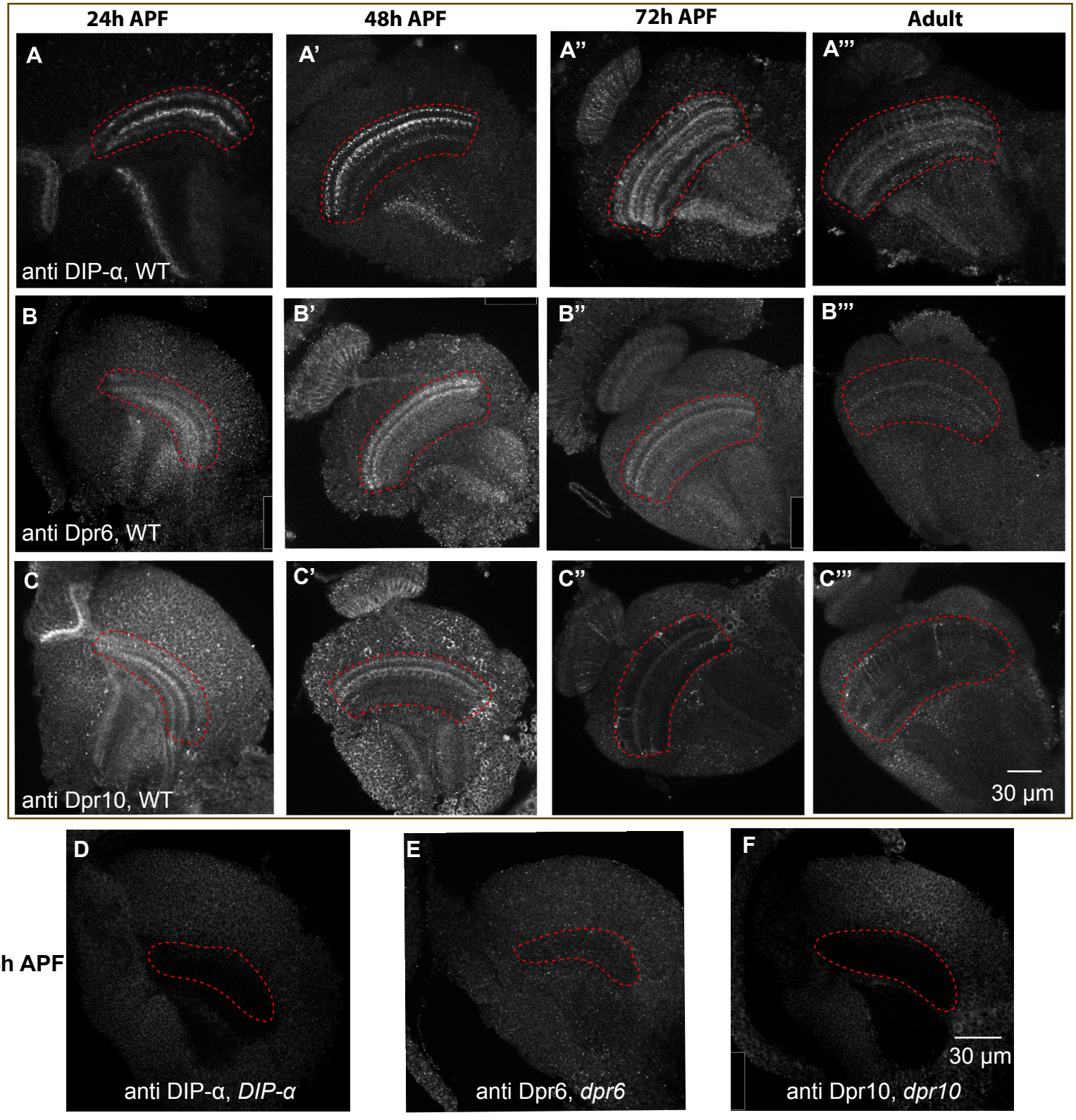
24h APF
48h APF
72h APF
Adult
A
A'
A''
A'''
anti DIP-α, WT
B
B'
B''
B'''
anti Dpr6, WT
C
C'
C''
C'''
anti Dpr10, WT
30 μm
24h APF
D
E
F
anti DIP-α, *DIP-α*
anti Dpr6, *dpr6*
anti Dpr10, *dpr10*
30 μm

Figure S2

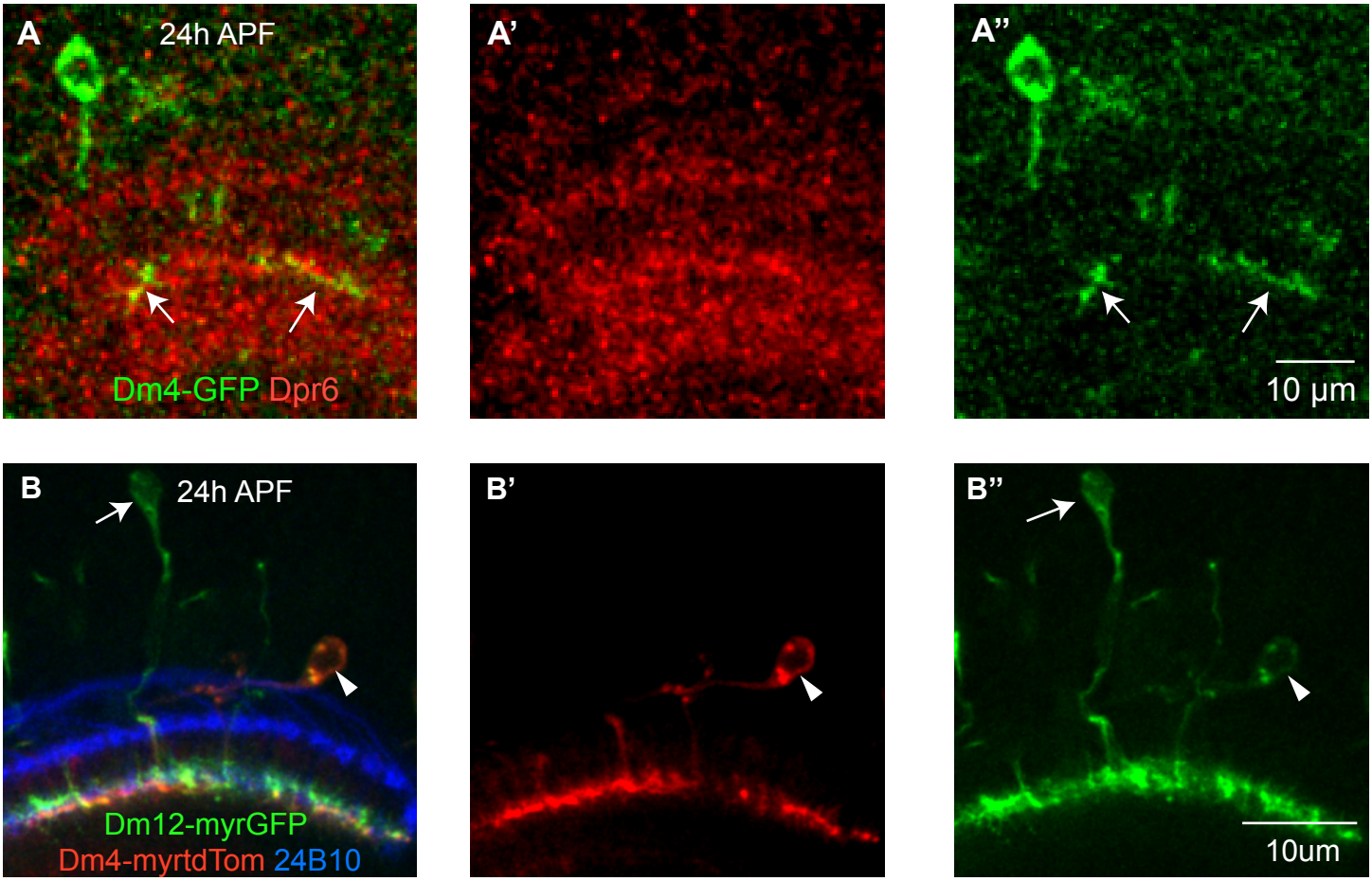
A
24h APF
Dm4-GFP Dpr6
A'
A''
10 µm
B
24h APF
Dm12-myrGFP
Dm4-myrtdTom 24B10
B'
B''
10um

Figure S3

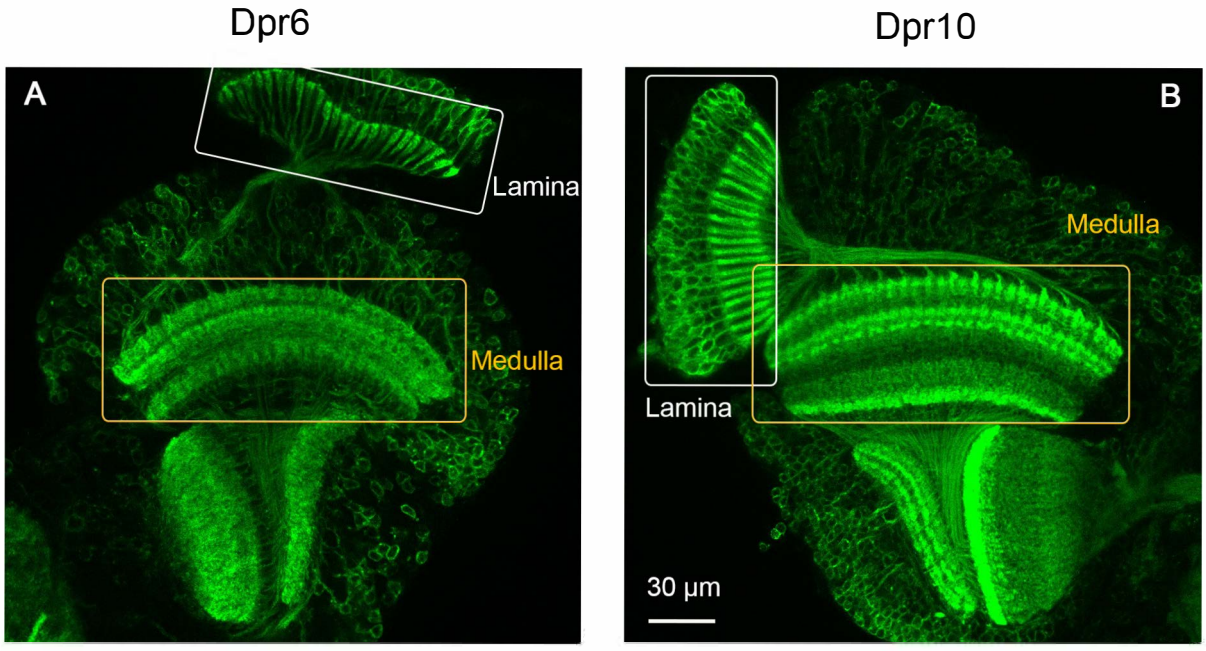

Figure S4

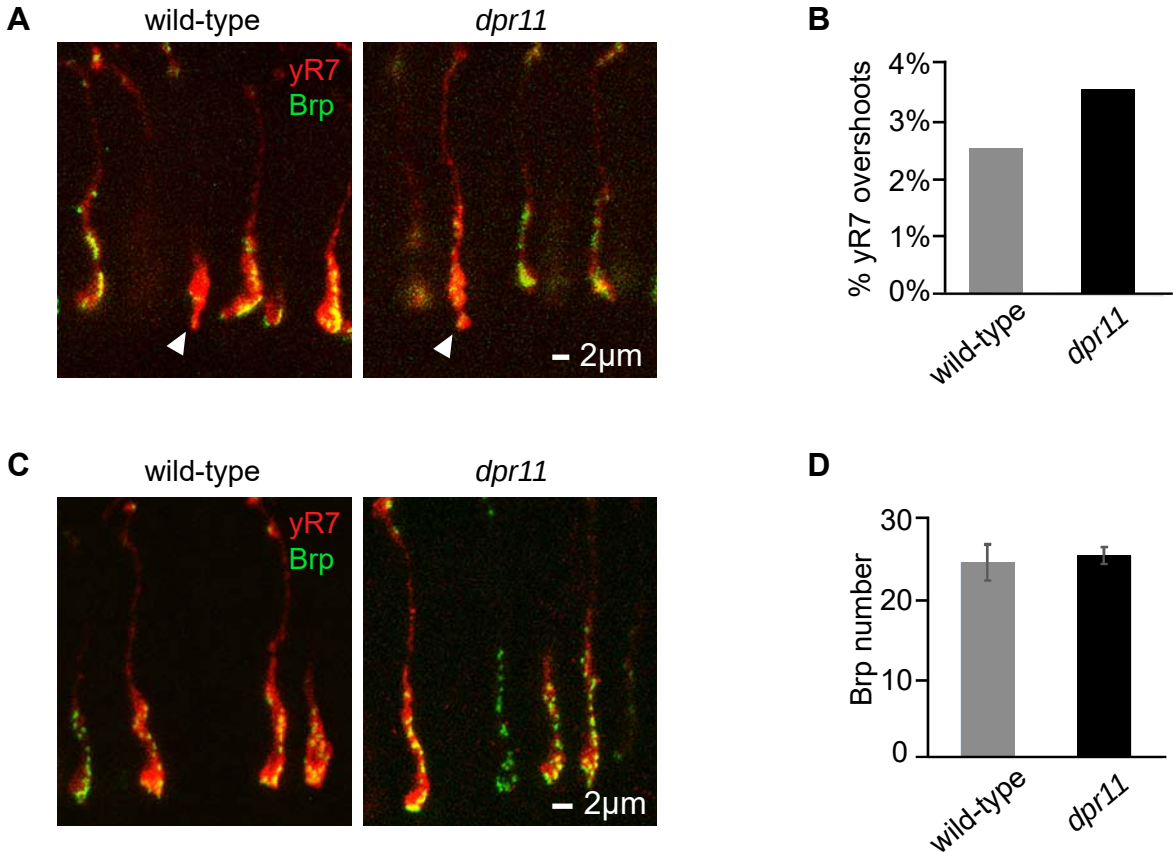
A
wild-type
dpr11
yR7
Brp
2µm
B
% yR7 overshoots
4%
3%
2%
1%
0%
wild-type
dpr11
C
wild-type
dpr11
yR7
Brp
2µm
D
Brp number
30
20
10
0
wild-type
dpr11

Figure S5

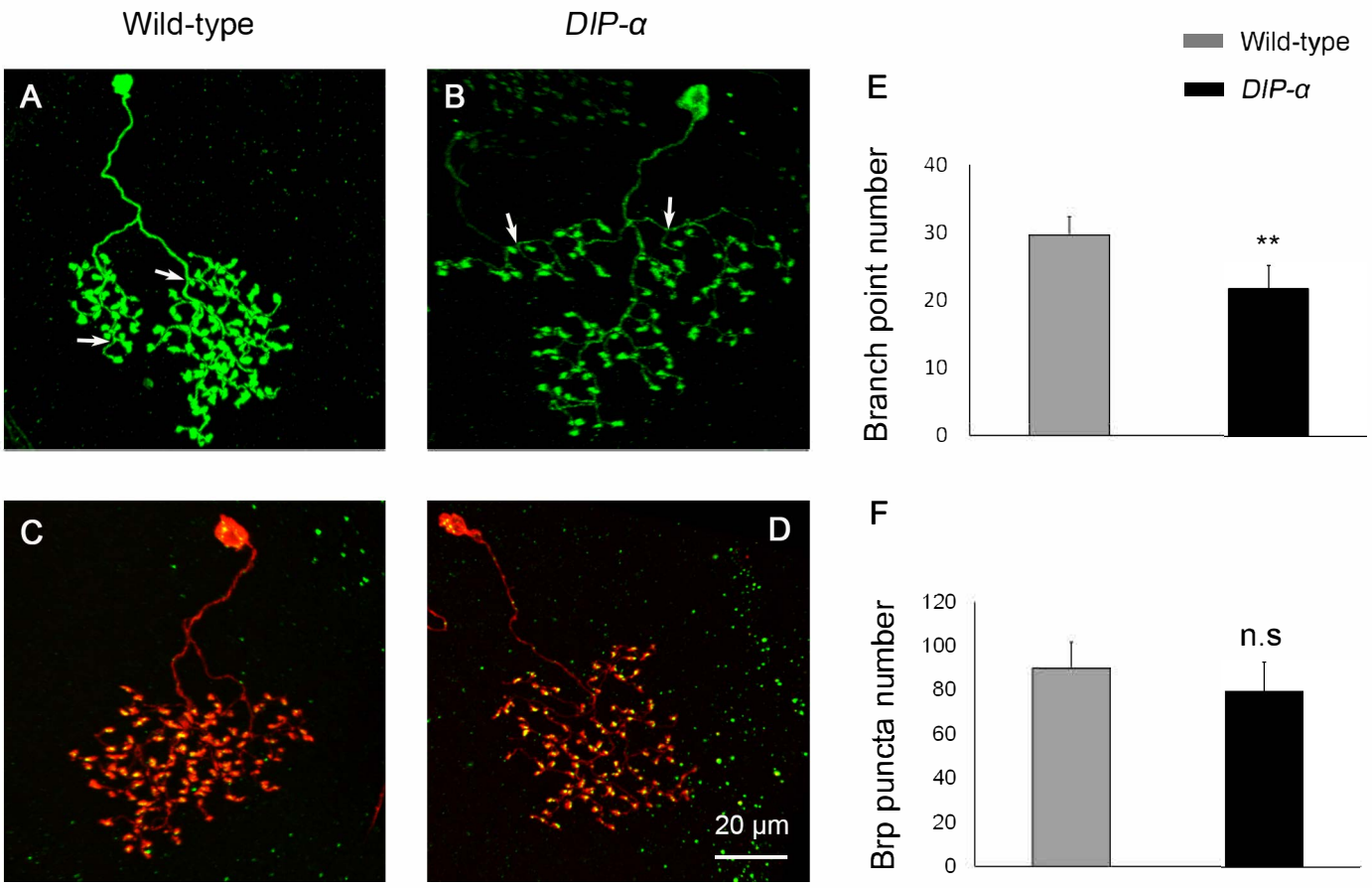
Wild-type
DIP-α
A
B
C
D
20 μm
E
Wild-type
DIP-α
Branch point number
40
30
20
10
0
**
F
Brp puncta number
120
100
80
60
40
20
0
n.s

Figure S6

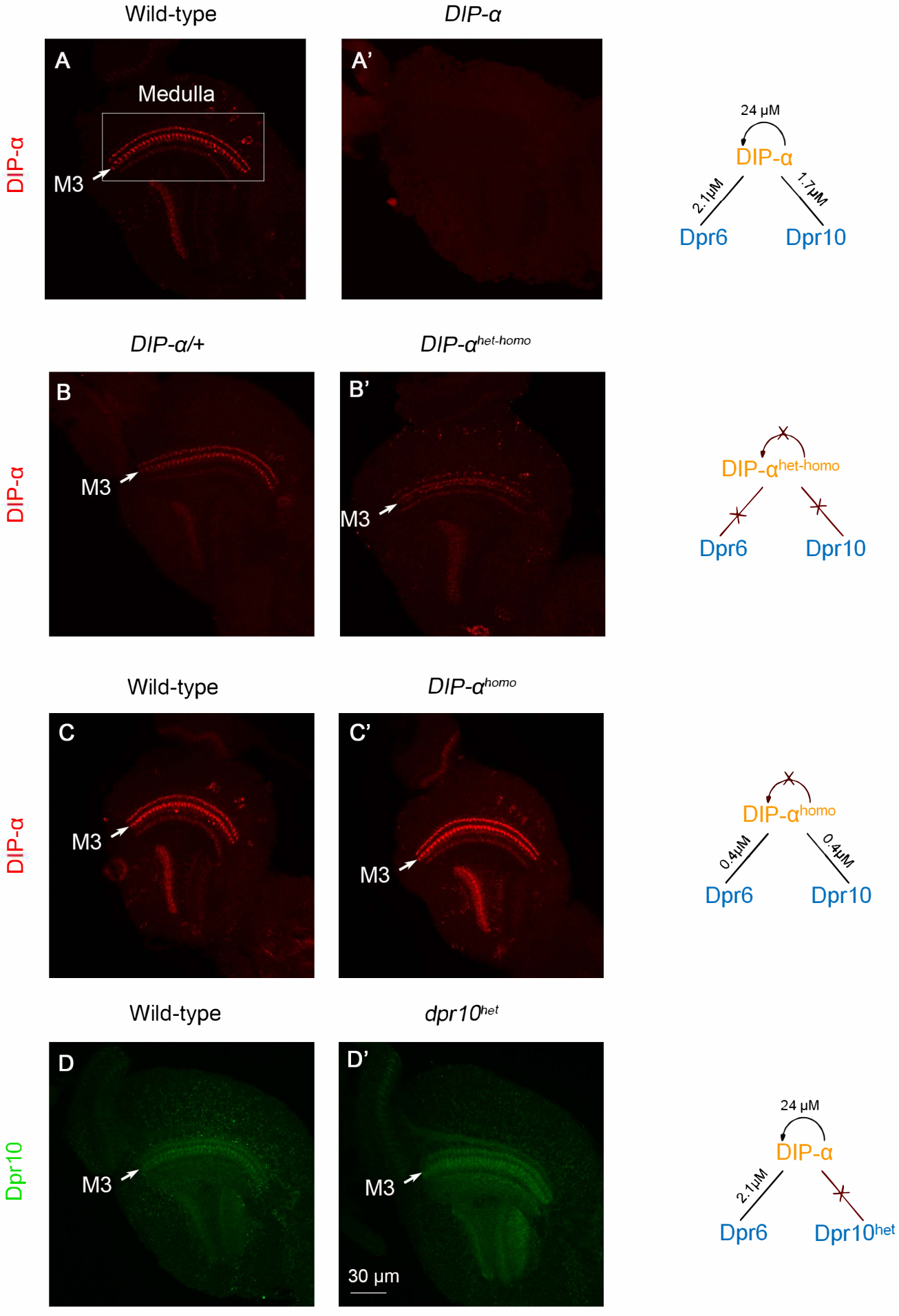
Wild-type
DIP-α
A
Medulla
M3
A'
DIP-α
24 μM
DIP-α
2.1μM
1.7μM
Dpr6
Dpr10
DIP-α/+
DIP-α^het-homo
B
M3
B'
M3
DIP-α
DIP-α^het-homo
Dpr6
Dpr10
Wild-type
DIP-α^homo
C
M3
C'
M3
DIP-α
DIP-α^homo
0.4μM
0.4μM
Dpr6
Dpr10
Wild-type
dpr10^het
D
M3
D'
M3
30 μm
Dpr10
24 μM
DIP-α
2.1μM
Dpr6
Dpr10^het

Figure S7

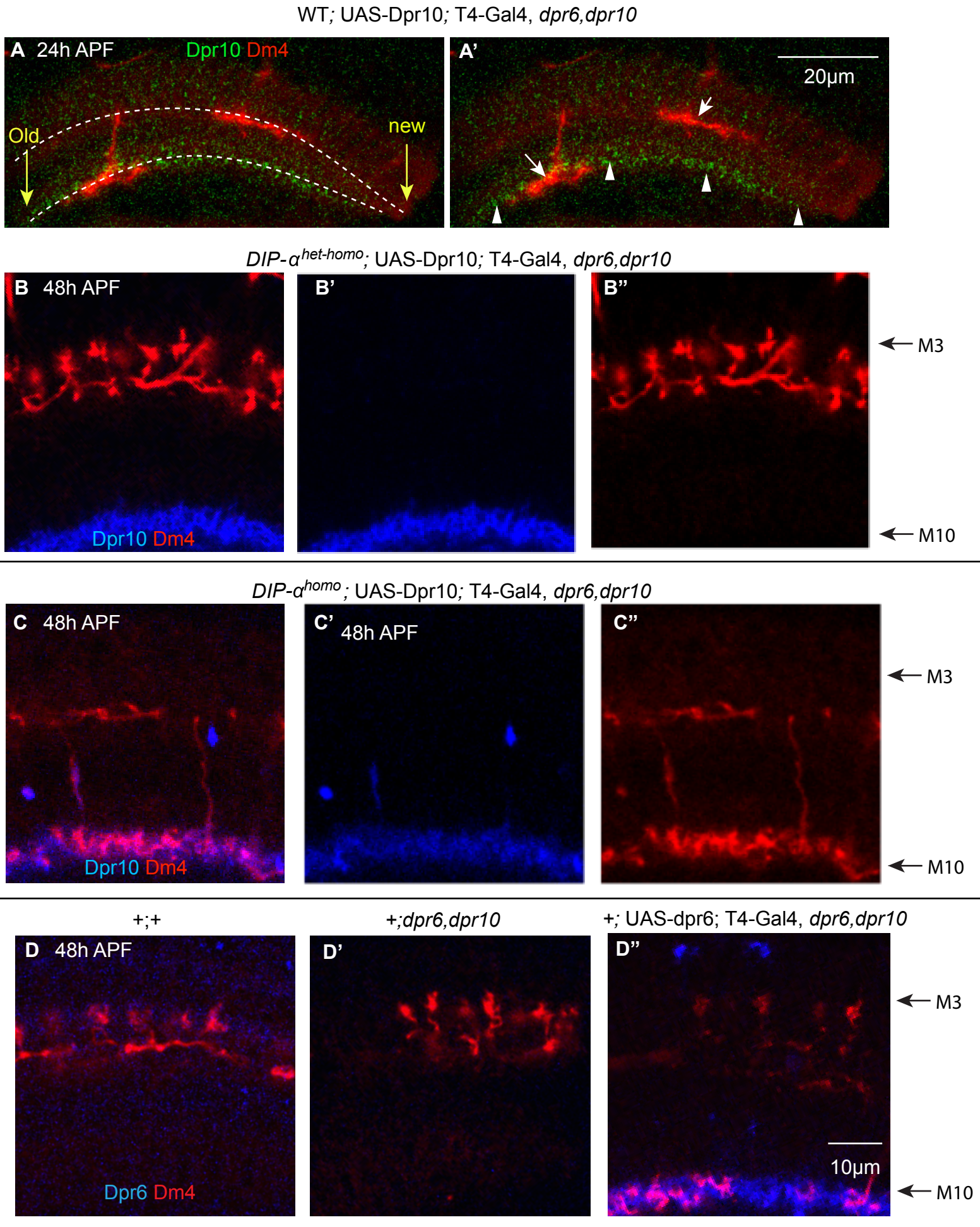
WT; UAS-Dpr10; T4-Gal4, dpr6,dpr10
A 24h APF
Dpr10 Dm4
Old
new
A'
20μm
DIP-α het-homo; UAS-Dpr10; T4-Gal4, dpr6,dpr10
B 48h APF
Dpr10 Dm4
B'
B"
M3
M10
DIP-α homo; UAS-Dpr10; T4-Gal4, dpr6,dpr10
C 48h APF
Dpr10 Dm4
C' 48h APF
C"
M3
M10
+;+
+;dpr6,dpr10
+; UAS-dpr6; T4-Gal4, dpr6,dpr10
D 48h APF
Dpr6 Dm4
D'
D"
10μm
M3
M10

Figure S8

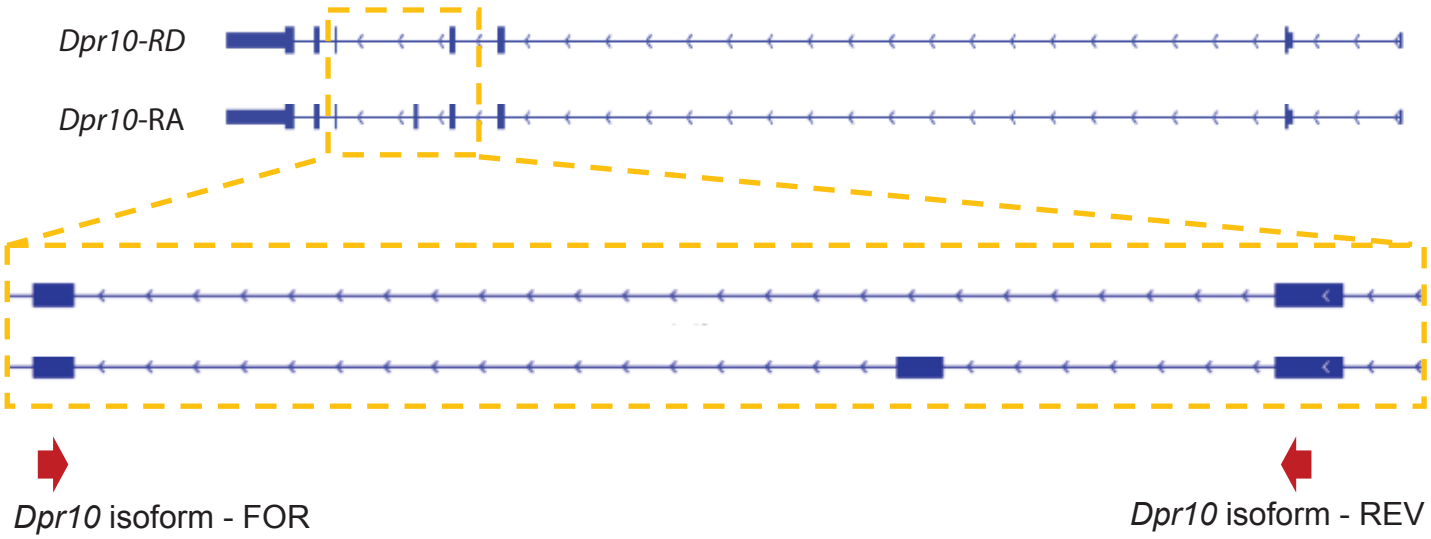

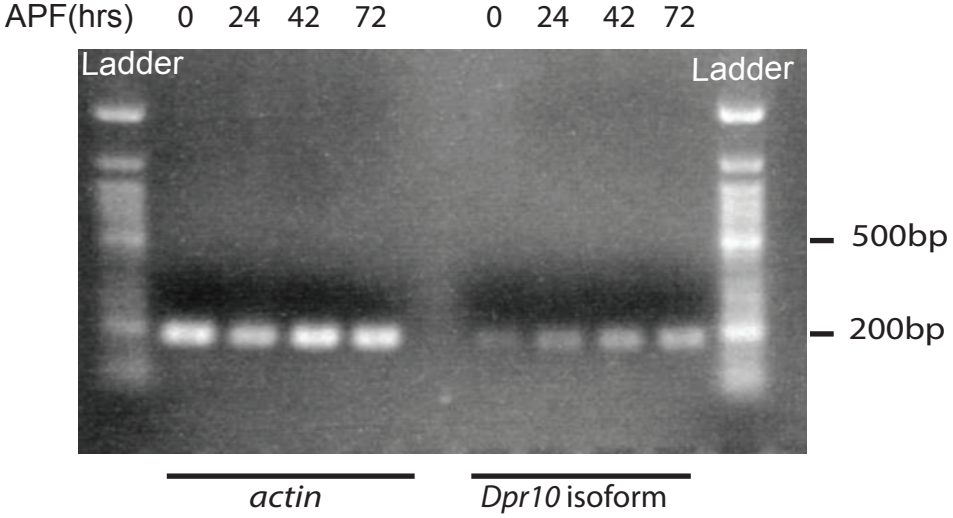

Expected PCR product size:

actin	190bp
Dpr10-RD	184bp
Dpr10-RA	322bp

Figure S9

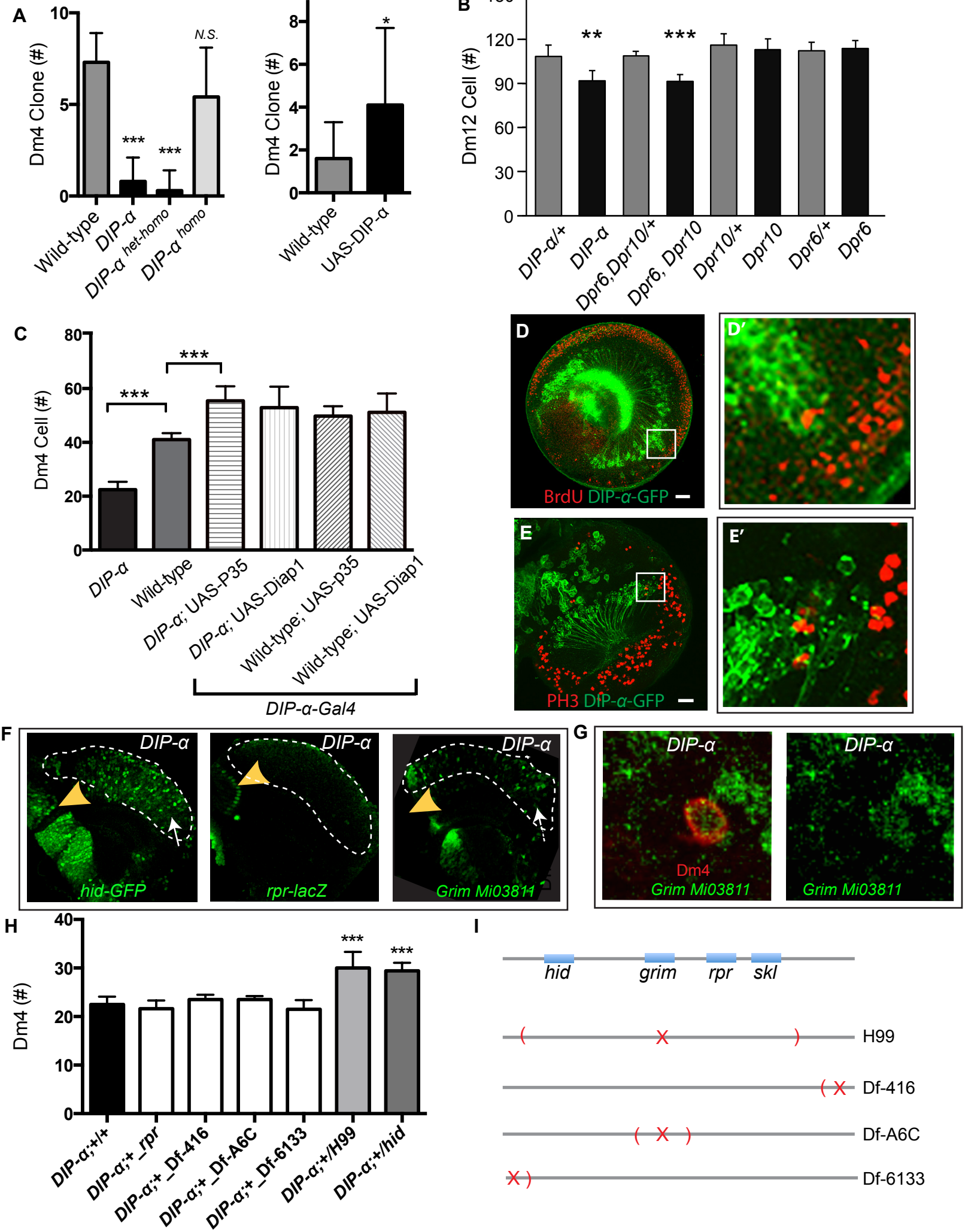
A
Dm4 Clone (#)
10
5
0
***
***
N.S.
Wild-type
DIP-α
DIP-α het-homo
DIP-α homo
Dm4 Clone (#)
8
6
4
2
0
*
Wild-type
UAS-DIP-α
B
Dm12 Cell (#)
150
120
90
60
30
0
**
***
DIP-α/+
DIP-α
Dpr6,Dpr10/+
Dpr6, Dpr10
Dpr10/+
Dpr10
Dpr6/+
Dpr6
C
Dm4 Cell (#)
80
60
40
20
0
***
***
DIP-α
Wild-type
DIP-α; UAS-P35
DIP-α; UAS-Diap1
Wild-type; UAS-p35
Wild-type; UAS-Diap1
DIP-α-Gal4
D
BrdU DIP-α-GFP
D′
E
PH3 DIP-α-GFP
E′
F
DIP-α
hid-GFP
DIP-α
rpr-lacZ
DIP-α
Grim Mi03811
G
DIP-α
Dm4
Grim Mi03811
DIP-α
Grim Mi03811
H
Dm4 (#)
40
30
20
10
0
***
***
DIP-α;+/+
DIP-α;+ _rpr
DIP-α;+ _Df-416
DIP-α;+ _Df-A6C
DIP-α;+ _Df-6133
DIP-α;+/H99
DIP-α;+/hid
I
hid
grim
rpr
skl
H99
Df-416
Df-A6C
Df-6133

Figure S10

A

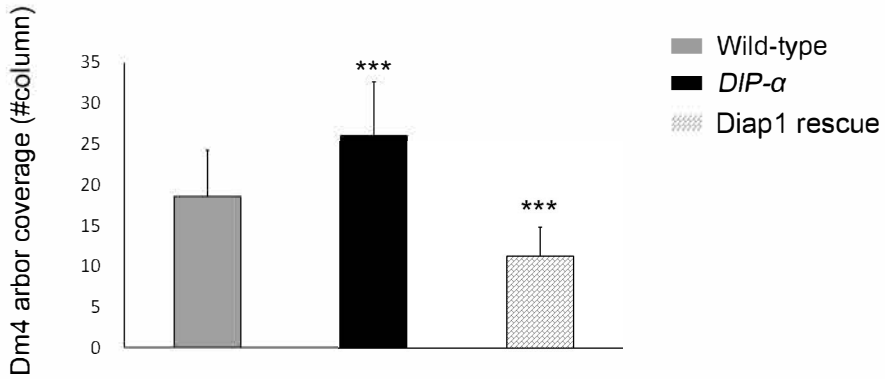

B

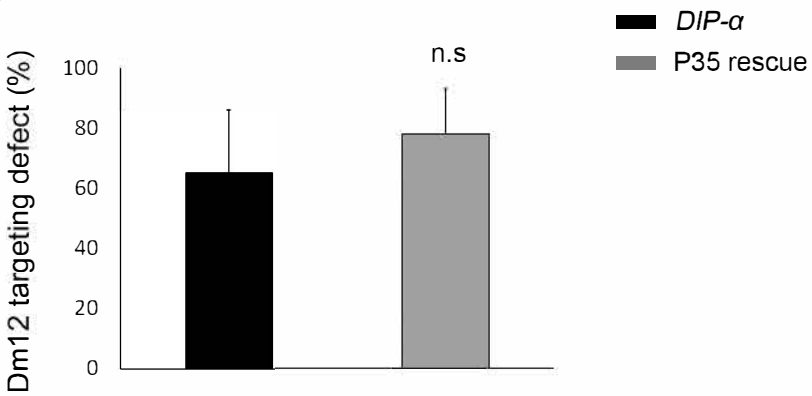

C

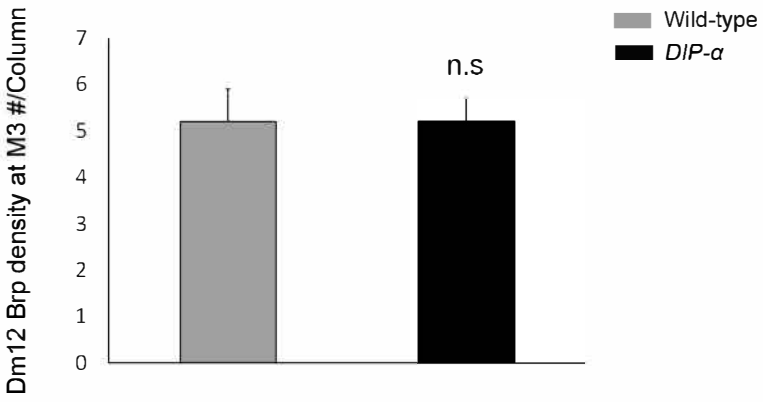

Figure S11

A

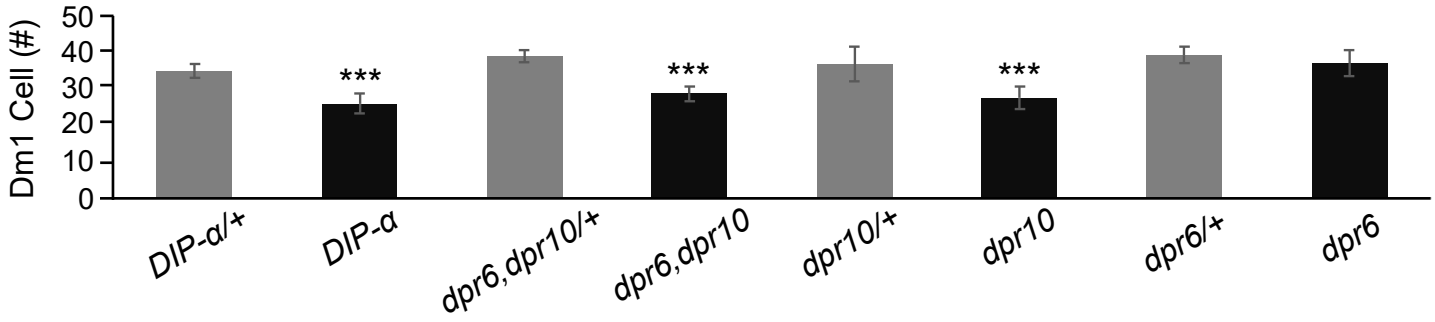

B

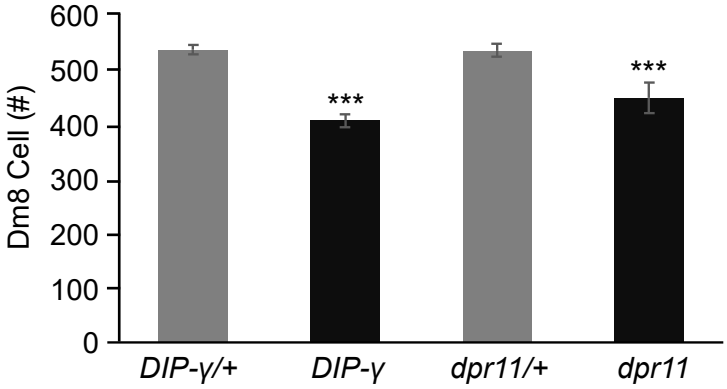

Figure S12

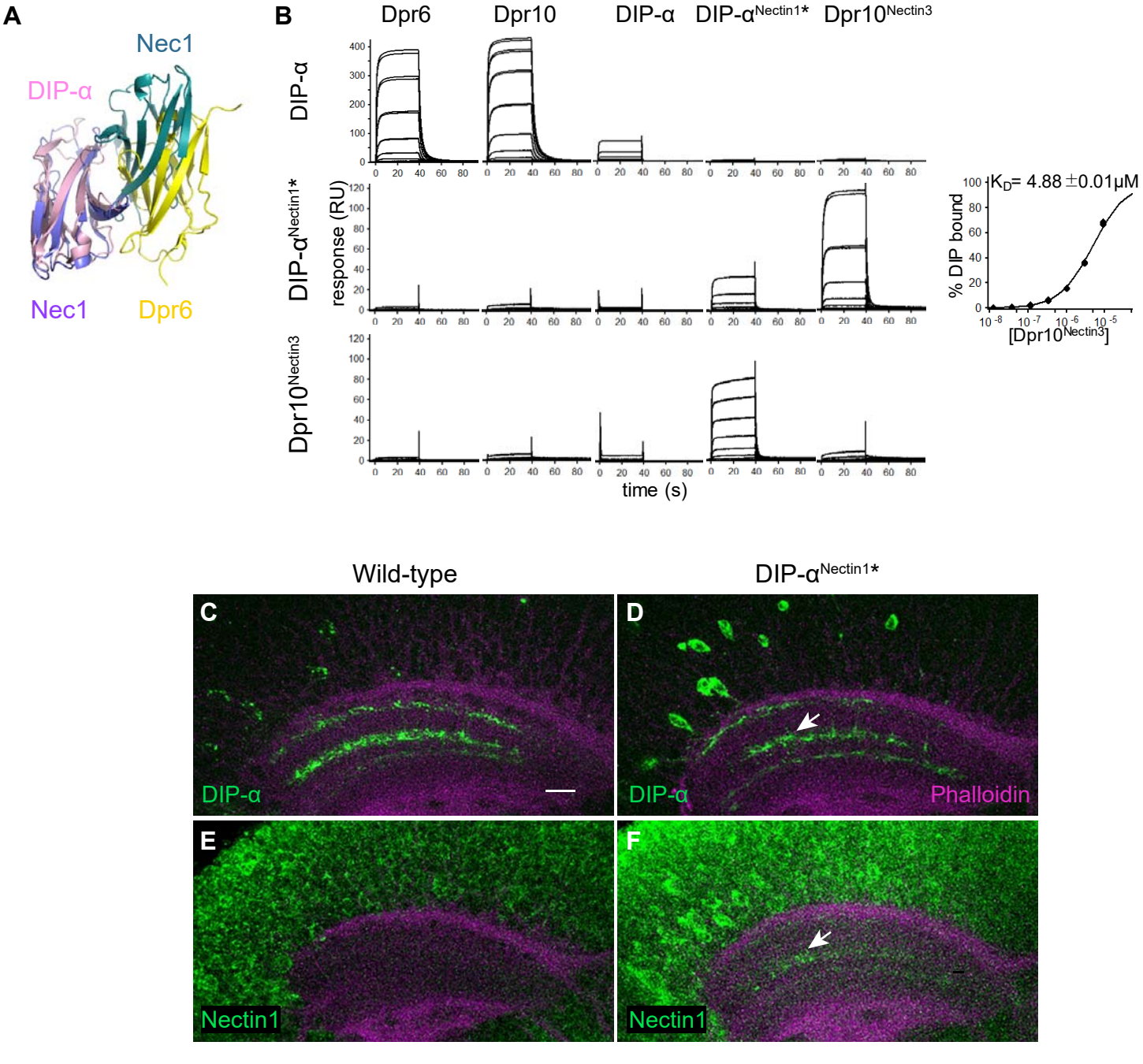
A
Nec1
DIP-α
Nec1
Dpr6
B
Dpr6
Dpr10
DIP-α
DIP-α^Nectin1*
Dpr10^Nectin3
DIP-α
DIP-α^Nectin1*
Dpr10^Nectin3
response (RU)
time (s)
K_D= 4.88 ±0.01μM
% DIP bound
[Dpr10^Nectin3]
Wild-type
DIP-α^Nectin1*
C
DIP-α
D
DIP-α
Phalloidin
E
Nectin1
F
Nectin1

Figure S13

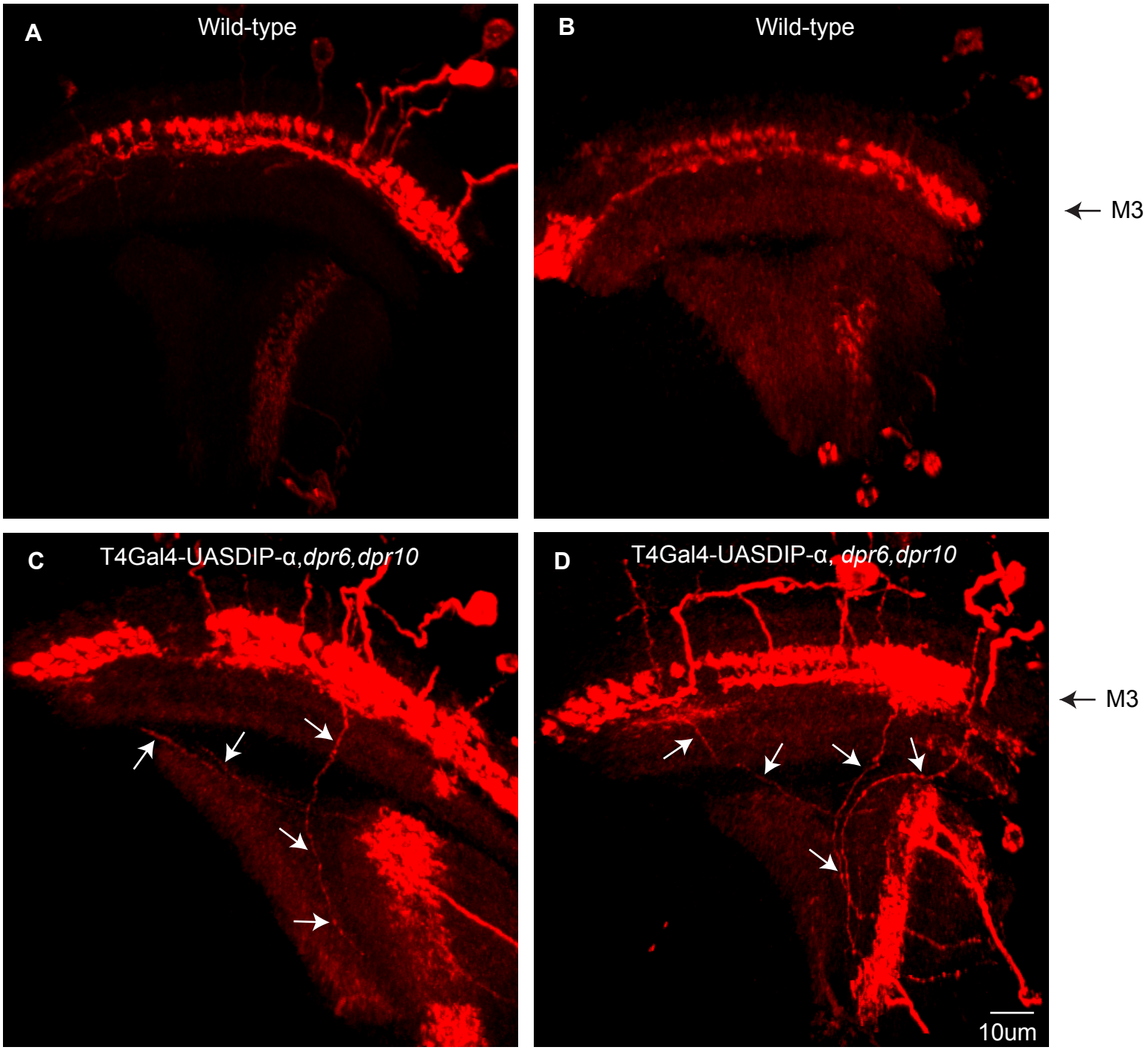
A
Wild-type
B
Wild-type
M3
C
T4Gal4-UASDIP-α,dpr6,dpr10
D
T4Gal4-UASDIP-α, dpr6,dpr10
M3
10um

Figure S14

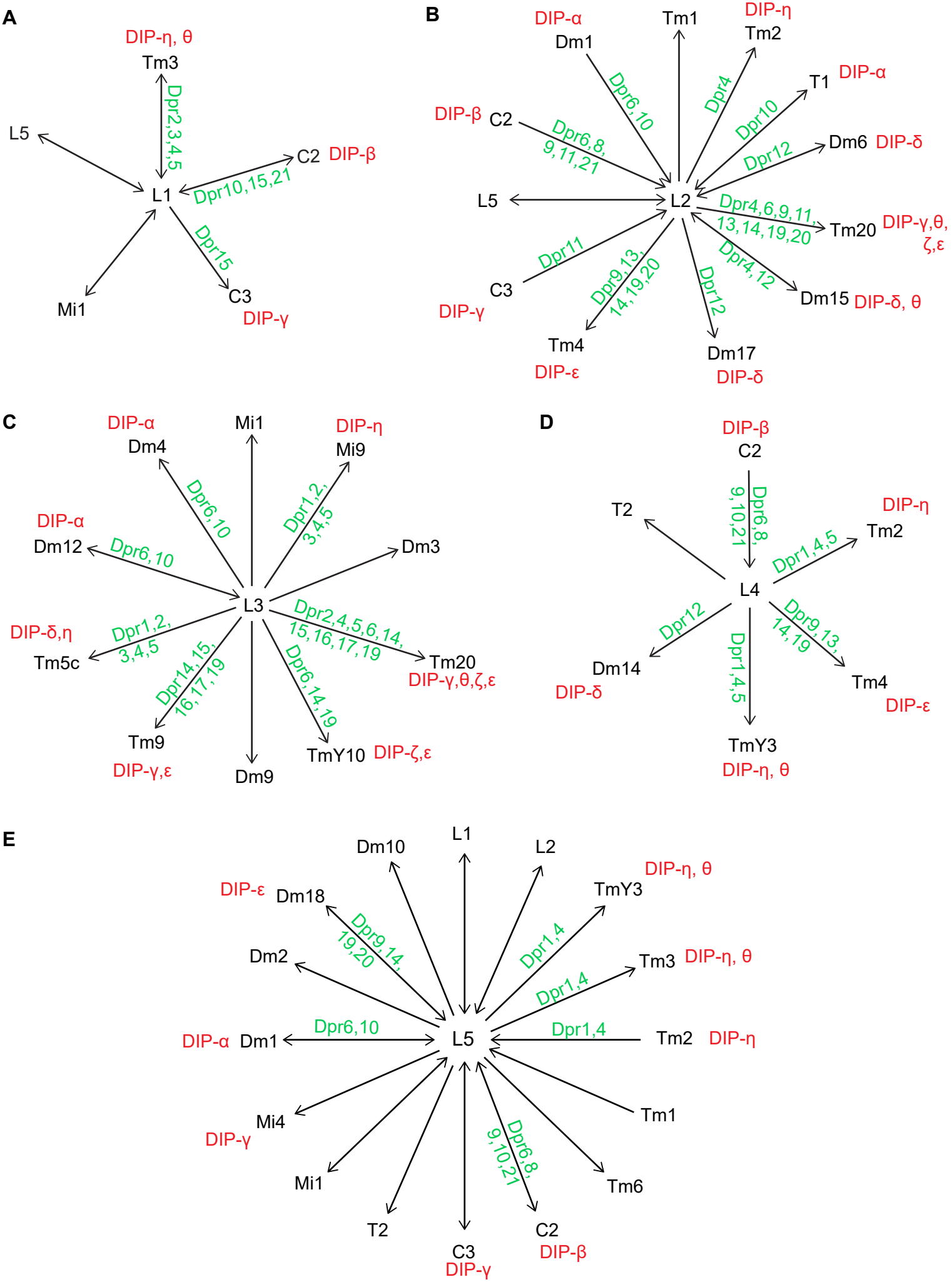
A
DIP-η, θ
Tm3
Dpr2,3,4,5
L5
C2
DIP-β
L1
Dpr10,15,21
Dpr15
Mi1
C3
DIP-γ
B
DIP-α
Dm1
Tm1
DIP-η
Tm2
Dpr6,10
Dpr4
T1
DIP-α
DIP-β
C2
Dpr10
Dpr6,8,9,11,21
Dpr12
Dm6
DIP-δ
L5
L2
Dpr4,6,9,11,13,14,19,20
Tm20
DIP-γ,θ,ζ,ε
Dpr11
Dpr4,12
C3
Dpr9,13,14,19,20
Dpr12
Dm15
DIP-δ, θ
DIP-γ
Tm4
Dm17
DIP-ε
DIP-δ
C
DIP-α
Dm4
Mi1
DIP-η
Mi9
Dpr6,10
Dpr1,2,3,4,5
DIP-α
Dm12
Dpr6,10
Dm3
L3
Dpr2,4,5,6,14,15,16,17,19
DIP-δ,η
Dpr1,2,3,4,5
Tm5c
Dpr14,15,16,17,19
Dpr6,14,19
Tm20
DIP-γ,θ,ζ,ε
Tm9
TmY10
DIP-ζ,ε
DIP-γ,ε
Dm9
D
DIP-β
C2
T2
Dpr6,8,9,10,21
DIP-η
Tm2
Dpr1,4,5
L4
Dpr12
Dpr9,13,14,19
Dpr1,4,5
Dm14
Tm4
DIP-δ
DIP-ε
TmY3
DIP-η, θ
E
L1
Dm10
L2
DIP-η, θ
DIP-ε
Dm18
TmY3
Dpr9,14,19,20
Dpr1,4
Dm2
Tm3
DIP-η, θ
Dpr1,4
Dpr6,10
Dpr1,4
DIP-α
Dm1
L5
Tm2
DIP-η
Tm1
Mi4
DIP-γ
Dpr6,8,9,10,21
Mi1
Tm6
T2
C2
C3
DIP-β
DIP-γ

Figure S15

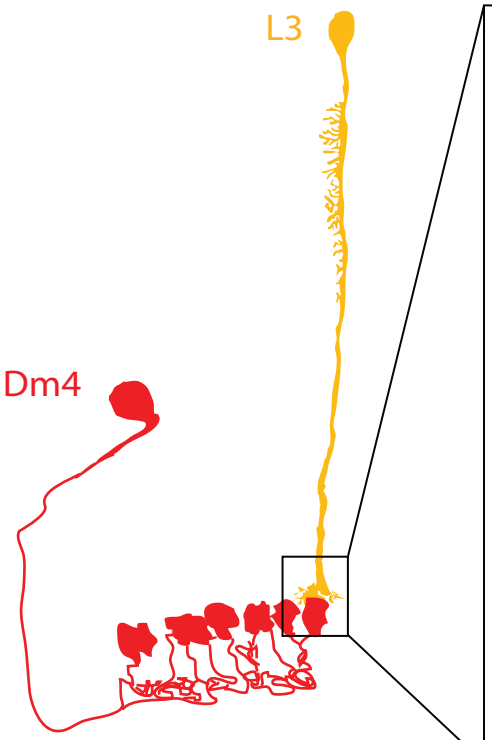

Interactors in Dm4	RPKM	Interactors in L3	RPKM
CG33543*	1080	Fas2	814
CG15630*	391	Fas2	814
klg*	306	klg	294
dpr7	298	dpr3	117
DIP-alpha*	123	dpr10	66
DIP-alpha*	123	dpr6	90
Dscam4	103	Dscam4	105
Dscam3	50	Dscam3	50
side-VII	45	beat-IV	60
NetB	33	fra	7
side-IV	29	18w	18
side-IV	29	beat-IIa	286
side-IV	29	beat-IIb	192
ed	28	tutl	279
ed	28	ed	12
Fas2	24	Fas2	814
Lac	23	Lac	179
tutl	22	ed	12
nrm	18	CG5597	5
Ptp99A	17	Ptp99A	96
fred	17	ed	12
fra	17	NetB	410
Fas3	10	Fas3	159
Tl	8	Tl	6
CG5597	6	nrm	22